Progress In Electromagnetics Research B, Vol. 31, 219–237, 2011

SPECTRAL-DOMAIN FORMULATION OF ELECTROMAGNETIC SCATTERING FROM CIRCULAR CYLINDERS LOCATED NEAR PERIODIC CYLINDER ARRAY

K. Watanabe [1, *] and Y. Nakatake [2]

[1]Department of Information and Communication Engineering, Fukuoka Institute of Technology, 3-30-1 Wajirohigashi, Higashi-ku, Fukuoka 811-0295, Japan

[2]Graduate School of Engineering, Fukuoka Institute of Technology, 3-30-1 Wajirohigashi, Higashi-ku, Fukuoka 811-0295, Japan

Abstract—This paper considers a periodic circular cylinder array with additional cylinders and formulates the electromagnetic scattering problem of this imperfectly periodic structure. Generally, the fields in imperfectly periodic structures have continuous spectra, and the spectral-domain approaches require appropriate discretization schemes in many cases. The present formulation is based on the pseudo-periodic Fourier transform and the discretization scheme can be considered only inside the Brillouin zone.

1. INTRODUCTION

Periodic structures are widely used in microwave, millimeter-wave, and optical wave regions, and many analytical and numerical approaches have been developed to analyze the scattering problems. The Floquet theorem asserts that, when a plane-wave illuminates a periodic structure, the scattered fields have discrete and equal interval spectra in the wavenumber space. This implies that the field components are pseudo-periodic (namely, each field component is a product of a periodic function and an exponential phase factor) and can be expressed in the generalized Fourier series expansions [1]. Also, the analysis region can be reduced to only one periodicity cell. However, when the incident field is not the plane-wave or the structural

Received 25 May 2011, Accepted 15 June 2011, Scheduled 22 June 2011
* Corresponding author: Koki Watanabe (koki@fit.ac.jp).

periodicity is collapsed even if locally, the Floquet theorem is no longer applicable and the analysis regions of the spatial-domain approaches have to generally cover all the scattering structure under consideration.

A spectral-domain formulation of the electromagnetic scattering from periodic structures with non-plane incident waves has been proposed in Ref. [2] by introducing the pseudo-periodic Fourier transform (PPFT). When the incident field is not the plane-wave, the fields in the periodic structures generally have continuous spectra in the wavenumber space, and an appropriate discretization is necessary for the spectral-domain approaches. PPFT is an extension of the periodic Green function [1], which is defined by the radiation field from periodic line-source array with phase shift, and converts any function to a pseudo-periodic function. The transformed incident field can be expressed in the plane-wave expansion and, therefore, the scattered fields for each plane wave incidence can be calculated by using the conventional approaches based on the Floquet theorem. PPFT introduces a transform parameter, which determines the wavenumber of each plane-wave, and the inverse transform is given by integrating with respect to the transform parameter over the Brillouin zone. It is well known that the fields in the periodic structures have infinite number of non-smooth points in the wavenumber space, which are called the Wood anomalies. However, PPFT makes us possible to consider an appropriate discretization scheme in the wavenumber space only inside the Brillouin zone.

This paper considers the two-dimensional electromagnetic scattering from some circular cylinders located near a periodic array of circular cylinders and presents a spectral-domain formulation based on the recursive transition-matrix algorithm (RTMA) [3] with the help of PPFT. The original RTMA is known as a very effective approach to the scattering from finite number of circular cylinders. It uses the cylindrical-wave expansions to express the field components and the boundary conditions at the cylinder surfaces are derived by Graf's addition theorem. RTMA with the lattice sums technique has been proposed for the scattering problem of a perfectly periodic cylinder array for plane-wave incidence [4], and a practical computation becomes possible by an integral representation of the lattice sums [5]. The present formulation applies the RTMA with the lattice sums technique to the scattering from the periodic cylinder array and the original RTMA to the scattering from the additional cylinders. The fields outside the cylinders are transformed by PPFT and the plane-wave amplitudes are matched by the technique for multilayer structure. The present formulation requires also an appropriate discretization in the Brillouin zone.

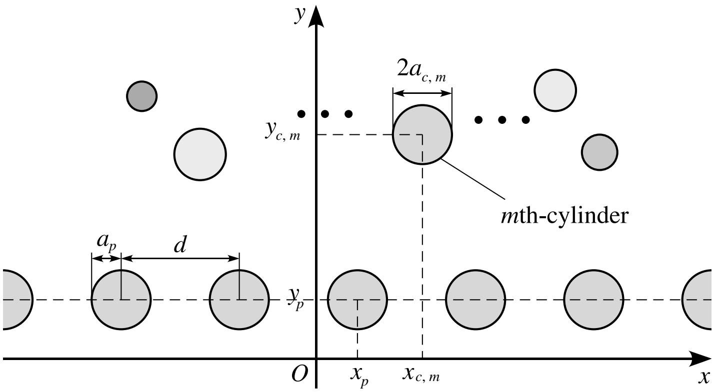

Figure 1. Structure under consideration.

2. SETTINGS OF THE PROBLEM

This paper considers the electromagnetic scattering problem of a circular cylinder array, in which a finite number of circular cylinders locates near a periodic array of circular cylinders schematically shown in Figure 1. All the cylinders are infinitely long in the z-direction and situated parallel to each other. The periodic cylinder array consists of identical cylinders with homogeneous and isotropic medium described by the permittivity ε_p and the permeability μ_p, and the radius is a_p. One cylinder in the periodic array is located at $(x, y) = (x_p, y_p)$ and the other cylinders are periodically spaced with a common distance d ($d > 2a_p$) in the x-direction. We denote $y_p + a_p$ and $y_p - a_p$ by $h_{p,1}$ and $h_{p,2}$, respectively. The number of cylinders located near the array is denoted by M, and the mth-cylinder ($m = 1, 2, \ldots, M$) is described by the permittivity $\varepsilon_{c,m}$, the permeability $\mu_{c,m}$, the radius $a_{c,m}$, and the center position $(x, y) = (x_{c,m}, y_{c,m})$. We denote $\max\{y_{c,m} + a_{c,m}\}$ and $\min\{y_{c,m} - a_{c,m}\}$ by $h_{c,1}$ and $h_{c,2}$, respectively. The parameters are chosen not to overlap each other and we suppose $h_{p,1} < h_{c,2}$. The surrounding region is filled by a lossless, homogeneous, and isotropic material with the permittivity ε_s and the permeability μ_s. The fields are supposed to be uniform in the z-direction and have a time-dependence in $\exp(-i\omega t)$. Therefore, two-dimensional problem is here considered, and two fundamental polarizations are expressed by TM and TE, in which the electric and magnetic fields are respectively perpendicular to the z-axis. We denote the z-component of electric field for TM-polarization and the z-component of magnetic for TE-polarization by $\psi(x, y)$, and show formulation for both polarizations simultaneously. The incident field is supposed to illuminate the scatterers from the upper or lower regions and there exists no source inside the scatterer region $h_{p,2} \leq y \leq h_{c,1}$.

3. TOOLS FOR THE FORMULATION

3.1. Pseudo-periodic Fourier Transform

The definition of PPFT and basic properties are presented in Ref. [2]. Let $f(x)$ be a function of x, and d be a positive real constant. Then the transform is defined by:

$$\bar{f}(x;\xi) = \sum_{m=-\infty}^{\infty} f(x - md)e^{imd\xi} \tag{1}$$

which is implicitly assumed to converge. This transform introduces a transform parameter ξ, and the inverse transform is formally given by integrating on ξ as

$$f(x) = \frac{1}{k_d} \int_{-k_d/2}^{k_d/2} \bar{f}(x;\xi)\, d\xi \tag{2}$$

where $k_d = 2\pi/d$. The transformed function $\bar{f}(x;\xi)$ has a pseudo-periodic property with the pseudo-period d in terms of x: $\bar{f}(x - md;\xi) = \bar{f}(x;\xi)e^{-imd\xi}$ for any integer m. Also, $\bar{f}(x;\xi)$ has a periodic property with the period k_d in terms of ξ: $\bar{f}(x;\xi - mk_d) = \bar{f}(x;\xi)$ for any integer m.

3.2. Expansion Bases

Since the region outside the cylinders is homogeneous, the fields transformed by PPFT can be expressed in the plane-wave expansions [2]. The basis functions of plane-wave expansion are here given by column matrices $\mathbf{f}^{(\pm)}(x, y;\xi)$, in which the nth-component is given as

$$\left(\mathbf{f}^{(\pm)}(x, y;\xi)\right)_n = e^{i(\alpha_n(\xi)x \pm \beta_n(\xi)y)} \tag{3}$$

with

$$\alpha_n(\xi) = \xi + nk_d \tag{4}$$

$$\beta_n(\xi) = \sqrt{{k_s}^2 - \alpha_n(\xi)^2} \tag{5}$$

where k_s denotes the wavenumber in the surrounding medium. The superscripts $(+)$ and $(-)$ indicate the column matrices corresponding to the plane-waves propagating in the positive and the negative y-direction, respectively. Let $(x, y) = (x_q, y_q)$ and $(x, y) = (x_r, y_r)$ be the reference points of the bases. Then the transform relation of the plane-wave bases is given as

$$\mathbf{f}^{(\pm)}(x-x_q, y-y_q; \xi) = \mathbf{F}(x_r-x_q, \pm(y_r-y_q); \xi)\,\mathbf{f}^{(\pm)}(x-x_r, y-y_r; \xi) \quad (6)$$

where $\mathbf{F}(x, y; \xi)$ denotes the diagonal matrices whose (n, m)-entries are given by

$$(\mathbf{F}(x, y; \xi))_{n,m} = \delta_{n,m} e^{i(\alpha_n(\xi)x+\beta_n(\xi)y)} \quad (7)$$

for the Kronecker delta $\delta_{n,m}$.

In the formulation, the cylindrical-wave expansions are also used to express the fields outside the cylinders. The bases functions are given by column matrices $\mathbf{g}^{(Z)}(x, y)$ whose nth-components are expressed as

$$\left(\mathbf{g}^{(Z)}(x, y)\right)_n = Z_n(k_s\rho(x, y))e^{in\phi(x,y)} \quad (8)$$

with

$$\rho(x, y) = \sqrt{x^2 + y^2} \quad (9)$$

$$\phi(x, y) = \arg(x + iy) \quad (10)$$

where Z specifies the cylindrical functions associating to the cylindrical-wave bases in such a way that $Z = J$ denotes the Bessel function and $Z = H^{(1)}$ denotes the Hankel function of the first kind. Graf's addition theorem [6] yields the transform relations for converting the reference points of the bases. Let (x_q, y_q) and (x_r, y_r) be the reference points of the cylindrical-wave bases. Then, when (x, y) is inside a circle with center (x_r, y_r) and radius $\rho(x_q - x_r, y_q - y_r)$, the transform relation is given by

$$\mathbf{g}^{(Z)}(x - x_q, y - y_q) = \mathbf{G}^{(Z)}(x_r - x_q, y_r - y_q)\mathbf{g}^{(J)}(x - x_r, y - y_r) \quad (11)$$

where $\mathbf{G}^{(Z)}(x, y)$ denotes the Toeplitz matrix whose (n, m)-entries are given by

$$\left(\mathbf{G}^{(Z)}(x, y)\right)_{n,m} = Z_{n-m}(k_s\rho(x, y))e^{i(n-m)\phi(x,y)}. \quad (12)$$

The plane-wave is known to be expressed by a superposition of the cylindrical-waves concerning with the Bessel function and the conversion relation is given as

$$\mathbf{f}^{(\pm)}(x, y; \xi) = \mathbf{A}^{(\pm)}(\xi)\mathbf{g}^{(J)}(x, y) \quad (13)$$

with

$$\left(\mathbf{A}^{(\pm)}(\xi)\right)_{n,m} = \left(\frac{i\alpha_n(\xi) \pm \beta_n(\xi)}{k_s}\right)^m. \quad (14)$$

Also, PPFT is applied to the cylindrical-waves concerning with the Hankel function of the first kind, and we can derive the following relation:

$$\sum_{l=-\infty}^{\infty} \mathbf{g}^{(H^{(1)})}(x-ld,y)e^{ild\xi} = \begin{cases} \mathbf{B}^{(+)}(\xi)\mathbf{f}^{(+)}(x,y;\xi) & \text{for} \quad y \geq 0 \\ \mathbf{B}^{(-)}(\xi)\mathbf{f}^{(-)}(x,y;\xi) & \text{for} \quad y < 0 \end{cases} \tag{15}$$

with

$$\left(\mathbf{B}^{(\pm)}(\xi)\right)_{n,m} = \frac{2}{d\beta_m(\xi)}\left(\frac{-i\alpha_m(\xi) \pm \beta_m(\xi)}{k_s}\right)^n \tag{16}$$

3.3. Transition-matrix of Isolated Cylinder

Here, we assume that one cylindrical scatterer is located at the origin. The permittivity and the permeability of the surrounding medium are ε_s and μ_s, respectively, and the cylinder is with radius a_m, permittivity ε_m, and permeability μ_m. An incident fields $\psi^{(i)}(x,y)$, which are expanded in series of cylindrical waves concerning with the Bessel functions as

$$\psi^{(i)}(x,y) = \mathbf{g}^{(J)}(x,y)^t\mathbf{a}^{(i)}, \tag{17}$$

illuminates the cylinder. The superscript t denotes the transpose and $\mathbf{a}^{(i)}$ is a column matrix generated by the expansion coefficients. Since the scattered field from the cylinder consists of the outgoing waves, it can be expressed in

$$\psi^{(s)}(x,y) = \mathbf{g}^{(H^{(1)})}(x,y)^t\mathbf{a}^{(s)} \tag{18}$$

where $\mathbf{a}^{(s)}$ is a column matrix generated by the expansion coefficients. Then, the transition-matrix (T-matrix) $\mathbf{T}_m$ is defined to relate the coefficients of incident and scattered fields in the following form:

$$\mathbf{a}^{(s)} = \mathbf{T}_m\mathbf{a}^{(i)}. \tag{19}$$

The (n,l)-components of $\mathbf{T}_m$ are given by

$$(\mathbf{T}_m)_{n,l} = \delta_{n,l}\frac{\zeta_s J_n(k_s a_m)J_n'(k_m a_m) - \zeta_m J_n'(k_s a_m)J_n(k_m a_m)}{\zeta_m H_n^{(1)'}(k_s a_m)J_n(k_m a_m) - \zeta_s H_n^{(1)}(k_s a_m)J_n'(k_m a_m)} \tag{20}$$

for TM-polarization, and

$$(\mathbf{T}_m)_{n,l} = \delta_{n,l}\frac{\zeta_m J_n(k_s a_m)J_n'(k_m a_m) - \zeta_s J_n'(k_s a_m)J_n(k_m a_m)}{\zeta_s H_n^{(1)'}(k_s a_m)J_n(k_m a_m) - \zeta_m H_n^{(1)}(k_s a_m)J_n'(k_m a_m)} \tag{21}$$

for TE-polarization, where ζ_m and ζ_s denote the characteristic impedances of the cylinder and the surrounding media, respectively, and k_m denotes the wavenumber in the cylinder medium. In the following formulation, the subscript "m" is replaced by "p" for the cylinders in the periodic cylinder array and "c, m" for the mth-cylinder in the additional cylinders.

4. FORMULATION

4.1. Scattering by Periodic Cylinder Array

This subsection presents a derivation process for the scattering-matrix (S-matrix) of the periodic cylinder array. Since no source exists in $h_{p,1} \geq y \geq h_{p,2}$, the incident field for the periodic array $\psi_p^{(i)}(x, y)$ consists of the waves propagating in the negative y-direction from the plane $y = h_{p,1}$ and the waves propagating in the positive y-direction from the plane $y = h_{p,2}$. Therefore, the incident field transformed by PPFT is given in the plane-wave expansion as

$$\bar{\psi}_p^{(i)}(x; \xi, y) = \mathbf{f}^{(-)}(x, y - h_{p,1}; \xi)^t \bar{\boldsymbol{\psi}}^{(-)}(\xi, h_{p,1}) + \mathbf{f}^{(+)}(x, y - h_{p,2}; \xi)^t \bar{\boldsymbol{\psi}}^{(+)}(\xi, h_{p,2}) \tag{22}$$

where $\bar{\psi}^{(+)}(\xi, y)$ and $\bar{\psi}^{(-)}(\xi, y)$ denote the column matrices of the amplitudes corresponding to the plane-waves propagating in the positive and the negative y-directions, respectively. Applying the inverse transform given by Equation (2) and using the relations (6) and (13), the incident field $\psi_p^{(i)}(x, y)$ is expressed in the cylindrical-wave expansion for the reference point $(x, y) = (x_p + \nu d, y_p)$ (center of the νth-cylinder) as

$$\psi_p^{(i)}(x, y) = \mathbf{g}^{(J)}(x - x_p - \nu d, y - y_p)^t \mathbf{a}_{p,\nu}^{(i)} \tag{23}$$

where the coefficient matrix $\mathbf{a}_{p,\nu}^{(i)}$ is given by

$$\mathbf{a}_{p,\nu}^{(i)} = \frac{1}{k_d} \int_{-k_d/2}^{k_d/2} \bar{\mathbf{a}}_p^{(i)}(\xi) e^{i\nu d\xi} d\xi \tag{24}$$

with

$$\bar{\mathbf{a}}_p^{(i)}(\xi) = \mathbf{A}^{(-)}(\xi)^t \mathbf{F}(x_p, a_p; \xi) \bar{\boldsymbol{\psi}}^{(-)}(\xi, h_{p,1}) + \mathbf{A}^{(+)}(\xi)^t \mathbf{F}(x_p, a_p; \xi) \bar{\boldsymbol{\psi}}^{(+)}(\xi, h_{p,2}). \tag{25}$$

On the other hand, the scattered field for the periodic array $\psi_p^{(s)}(x, y)$ consists of the outward propagating waves from the cylinders, and the scattered field outside the cylinders is given in the following form:

$$\psi_p^{(s)}(x, y) = \sum_{l=-\infty}^{\infty} \mathbf{g}^{(H^{(1)})}(x - x_p - ld, y - y_p)^t \mathbf{a}_{p,l}^{(s)} \tag{26}$$

where $\mathbf{a}_{p,l}^{(s)}$ denotes the column matrix generated by the expansion coefficients of the scattered waves from the lth-cylinder. Applying

PPFT to the scattered field and using the relations (15) and (6), we may obtain

$$\bar{\psi}_p^{(s)}(x;\xi,y) = \begin{cases} \mathbf{f}^{(+)}(x,y-h_{p,1};\xi)^t\mathbf{F}(-x_p,a_p;\xi)\mathbf{B}^{(+)}(\xi)^t\bar{\mathbf{a}}_p^{(s)}(\xi) & \text{for } y\geq h_{p,1} \\ \mathbf{f}^{(-)}(x,y-h_{p,2};\xi)^t\mathbf{F}(-x_p,a_p;\xi)\mathbf{B}^{(-)}(\xi)^t\bar{\mathbf{a}}_p^{(s)}(\xi) & \text{for } y\leq h_{p,2} \end{cases} \tag{27}$$

where the column matrix $\bar{\mathbf{a}}_p^{(s)}(\xi)$ is defined by

$$\bar{\mathbf{a}}_p^{(s)}(\xi) = \sum_{\nu=-\infty}^{\infty} \mathbf{a}_{p,\nu}^{(s)} e^{-i\nu d\xi}. \tag{28}$$

Using Equation (11), the total field near but outside the νth-cylinder can be expressed as

$$\begin{aligned}\psi(x,y) &= \mathbf{g}^{(J)}(x-x_p-\nu d, y-y_p)^t \left(\mathbf{a}_{p,\nu}^{(i)} + \sum_{\substack{l\neq\nu \\ l=-\infty}}^{\infty} \mathbf{G}^{(H^{(1)})}((\nu-l)d,0)^t \mathbf{a}_{p,l}^{(s)}\right) \\ &\quad + \mathbf{g}^{(H^{(1)})}(x-x_p-\nu d, y-y_p)^t \mathbf{a}_{p,\nu}^{(s)}. \end{aligned} \tag{29}$$

The first and the second terms on the right-hand side of Equation (29) are given by superpositions of cylindrical-waves associating to the Bessel function and the Hankel function of the first kind, respectively, and they represent the incident and the scattered fields for the νth-cylinder. As shown in the Subsection 3.3, the T-matrix $\mathbf{T}_p$ provides a relation between the coefficient matrices of the incident and the scattered fields, and we have

$$\mathbf{a}_{p,\nu}^{(s)} = \mathbf{T}_p \left(\mathbf{a}_{p,\nu}^{(i)} + \sum_{\substack{l\neq\nu \\ l=-\infty}}^{\infty} \mathbf{G}^{(H^{(1)})}((\nu-l)d,0)^t \mathbf{a}_{p,l}^{(s)}\right). \tag{30}$$

Multiplying an exponential function $\exp(-i\nu d\xi)$ to Equation (30) and summing over all integers ν, we may obtain the following relation:

$$\bar{\mathbf{a}}_p^{(s)}(\xi) = \left(\mathbf{T}_p^{-1} - \mathbf{L}(\xi)\right)^{-1} \bar{\mathbf{a}}_p^{(i)}(\xi) \tag{31}$$

with

$$\mathbf{L}(\xi) = \sum_{\substack{l\neq\nu \\ l=-\infty}}^{\infty} \mathbf{G}^{(H^{(1)})}(-\nu d,0)^t e^{i\nu d\xi}. \tag{32}$$

We consider the total field at $y = h_{p,1}, h_{p,2}$ in the plane-wave expansion representation, and use Equations (25), (27), and (31). Then, the relations between the amplitudes of the incoming and the outgoing plane-waves as

$$\begin{pmatrix} \bar{\boldsymbol{\psi}}^{(+)}(\xi, h_{p,1}) \\ \bar{\boldsymbol{\psi}}^{(-)}(\xi, h_{p,2}) \end{pmatrix} = \left[\begin{pmatrix} \mathbf{0} & \mathbf{F}(0, 2a_p; \xi) \\ \mathbf{F}(0, 2a_p; \xi) & \mathbf{0} \end{pmatrix} + \begin{pmatrix} \bar{\mathbf{S}}_{p,11}(\xi) & \bar{\mathbf{S}}_{p,12}(\xi) \\ \bar{\mathbf{S}}_{p,21}(\xi) & \bar{\mathbf{S}}_{p,22}(\xi) \end{pmatrix} \right] \begin{pmatrix} \bar{\boldsymbol{\psi}}^{(-)}(\xi, h_{p,1}) \\ \bar{\boldsymbol{\psi}}^{(+)}(\xi, h_{p,2}) \end{pmatrix} \tag{33}$$

with

$$\bar{\mathbf{S}}_{p,11}(\xi) = \mathbf{F}(-x_p, a_p; \xi) \mathbf{B}^{(+)}(\xi)^t \left(\mathbf{T}_p^{-1} - \mathbf{L}(\xi) \right)^1 \mathbf{A}^{(-)}(\xi)^t \mathbf{F}(x_p, a_p; \xi) \tag{34}$$

$$\bar{\mathbf{S}}_{p,12}(\xi) = \mathbf{F}(-x_p, a_p; \xi) \mathbf{B}^{(+)}(\xi)^t \left(\mathbf{T}_p^{-1} - \mathbf{L}(\xi) \right)^{-1} \mathbf{A}^{(+)}(\xi)^t \mathbf{F}(x_p, a_p; \xi) \tag{35}$$

$$\bar{\mathbf{S}}_{p,21}(\xi) = \mathbf{F}(-x_p, a_p; \xi) \mathbf{B}^{(-)}(\xi)^t \left(\mathbf{T}_p^{-1} - \mathbf{L}(\xi) \right)^{-1} \mathbf{A}^{(-)}(\xi)^t \mathbf{F}(x_p, a_p; \xi) \tag{36}$$

$$\bar{\mathbf{S}}_{p,22}(\xi) = \mathbf{F}(-x_p, a_p; \xi) \mathbf{B}^{(-)}(\xi)^t \left(\mathbf{T}_p^{-1} - \mathbf{L}(\xi) \right)^{-1} \mathbf{A}^{(+)}(\xi)^t \mathbf{F}(x_p, a_p; \xi). \tag{37}$$

4.2. Scattering by Additional Cylinders

Next, we consider the scattering from the additional cylinders located near the periodic array by applying original RTMA. Here, we denote the incident field for the additional cylinders by $\psi_c^{(i)}(x, y)$ and express the transformed field in the plane-wave expansion as

$$\bar{\psi}_c^{(i)}(x; \xi, y) = \mathbf{f}^{(-)}(x, y - h_{c,1}; \xi)^t \bar{\boldsymbol{\psi}}^{(-)}(\xi, h_{c,1}) + \mathbf{f}^{(+)}(x, y - h_{c,2}; \xi)^t \bar{\boldsymbol{\psi}}^{(+)}(\xi, h_{c,2}). \tag{38}$$

This expression is inversely transformed and Equations (6) and (13) are used. Then we have the cylindrical-wave expansion representation of the incident field for the reference point $(x, y) = (x_{c,\nu}, y_{c,\nu})$ as

$$\psi_c^{(i)}(x, y) = \mathbf{g}^{(J)}(x - x_{c,\nu}, y - y_{c,\nu})^t \mathbf{a}_{c,\nu}^{(i)} \tag{39}$$

where the coefficient matrix $\mathbf{a}_{c,\nu}^{(i)}$ is given by

$$\mathbf{a}_{c,\nu}^{(i)} = \frac{1}{k_d}\int_{-k_d/2}^{k_d/2}\Big(\mathbf{A}^{(-)}(\xi)^t\mathbf{F}(x_{c,\nu}, h_{c,1}-y_{c,\nu};\xi)\bar{\boldsymbol{\psi}}^{(-)}(\xi, h_{c,1}) + \mathbf{A}^{(+)}(\xi)^t\mathbf{F}(x_{c,\nu}, y_{c,\nu}-h_{c,2};\xi)\bar{\boldsymbol{\psi}}^{(+)}(\xi, h_{c,2})\Big)\,d\xi. \quad (40)$$

The scattered field for the additional cylinders is given by the sum of the outgoing waves from the cylinders as

$$\psi_c^{(s)}(x,y) = \sum_{l=1}^{M}\mathbf{g}^{(H^{(1)})}(x-x_{c,l}, y-y_{c,l})^t\mathbf{a}_{c,l}^{(s)} \quad (41)$$

where $\mathbf{a}_{p,l}^{(i)}$ denotes the coefficient matrix corresponding to the scattered waves from the lth-cylinder. PPFT is applied to the scattered field and we may obtain

$$\bar{\psi}_c^{(s)}(x;\xi,y) = \begin{cases}\mathbf{f}^{(+)}(x, y-h_{c,1};\xi)^t\tilde{\mathbf{B}}_c^{(+)}(\xi)\tilde{\mathbf{a}}_c^{(s)} & \text{for} \quad y \geq h_{c,1}\\ \mathbf{f}^{(-)}(x, y-h_{c,2};\xi)^t\tilde{\mathbf{B}}_c^{(-)}(\xi)\tilde{\mathbf{a}}_c^{(s)} & \text{for} \quad y \leq h_{c,2}\end{cases} \quad (42)$$

by using the relations (6) and (15), where the matrices $\tilde{\mathbf{B}}_c^{(+)}(\xi)$ and $\tilde{\mathbf{B}}_c^{(-)}(\xi)$ are defined by

$$\tilde{\mathbf{B}}_c^{(\pm)}(\xi) = \Big(\mathbf{B}_1^{(\pm)\prime}(\xi) \quad \ldots \quad \mathbf{B}_M^{(\pm)\prime}(\xi)\Big) \quad (43)$$

with

$$\mathbf{B}_m^{(+)\prime}(\xi) = \mathbf{F}(-x_{c,m}, h_{c,1}-y_{c,m};\xi)\mathbf{B}^{(+)}(\xi)^t \quad (44)$$

$$\mathbf{B}_m^{(-)\prime}(\xi) = \mathbf{F}(-x_{c,m}, y_{c,m}-h_{c,2};\xi)\mathbf{B}^{(-)}(\xi)^t. \quad (45)$$

The relation (11) is applied to the scattered field given by Equation (41), and the total field near but outside the νth-cylinder is expressed as

$$\psi(x,y) = \mathbf{g}^{(J)}(x-x_{c,\nu}, y-y_{c,\nu})^t\left(\mathbf{a}_{c,\nu}^{(i)} + \sum_{\substack{m\neq\nu\\ m=1}}^{M}\mathbf{G}^{(H^{(1)})}(x_{c,\nu}-x_{c,m}, y_{c,\nu}-y_{c,m})^t\mathbf{a}_{c,m}^{(s)}\right) + \mathbf{g}^{(H^{(1)})}(x-x_{c,\nu}, y-y_{c,\nu})^t\mathbf{a}_{c,\nu}^{(s)}. \quad (46)$$

The coefficient matrices of the first and the second terms on the right-hand side are related by the T-matrix as

$$\mathbf{a}_{c,\nu}^{(s)} = \mathbf{T}_{c,\nu}\left(\mathbf{a}_{c,\nu}^{(i)} + \sum_{\substack{m\neq\nu\\ m=1}}^{M}\mathbf{G}^{(H^{(1)})}(x_{c,\nu}-x_{c,m}, y_{c,\nu}-y_{c,m})^t\mathbf{a}_{c,m}^{(s)}\right), \quad (47)$$

and this relation is also written as

$$\tilde{\mathbf{a}}_c^{(s)} = \tilde{\mathbf{C}}^{-1}\tilde{\mathbf{a}}_c^{(i)} \tag{48}$$

with

$$\tilde{\mathbf{a}}_c^{(f)} = \begin{pmatrix} \mathbf{a}_{c,1}^{(f)} \\ \vdots \\ \mathbf{a}_{c,M}^{(f)} \end{pmatrix} \tag{49}$$

$$\tilde{\mathbf{C}} = \begin{pmatrix} \mathbf{C}_{1,1} & \dots & \mathbf{C}_{1,M} \\ \vdots & \ddots & \vdots \\ \mathbf{C}_{M,1} & \dots & \mathbf{C}_{M,M} \end{pmatrix} \tag{50}$$

$$\mathbf{C}_{n,m} = \begin{cases} \mathbf{T}_{c,n}^{-1} & \text{for} \quad n = m \\ -\mathbf{G}^{(H^{(1)})}(x_{c,n} - x_{c,m}, y_{c,n} - y_{c,m})^t & \text{for} \quad n \neq m \end{cases} \tag{51}$$

for $f = i, s$. From Equations (40), (42), and (48), we may obtain the relations between the amplitudes of the incoming and the outgoing plane-waves in the following form:

$$\begin{aligned} &\begin{pmatrix} \bar{\boldsymbol{\psi}}^{(+)}(\xi, h_{c,1}) \\ \bar{\boldsymbol{\psi}}^{(-)}(\xi, h_{c,2}) \end{pmatrix} \\ &= \begin{pmatrix} \mathbf{0} & \mathbf{F}(0, h_{c,1} - h_{c,2}; \xi) \\ \mathbf{F}(0, h_{c,1} - h_{c,2}; \xi) & \mathbf{0} \end{pmatrix} \begin{pmatrix} \bar{\boldsymbol{\psi}}^{(-)}(\xi, h_{c,1}) \\ \bar{\boldsymbol{\psi}}^{(+)}(\xi, h_{c,2}) \end{pmatrix} \\ &+ \frac{1}{k_d}\int_{-k_d/2}^{k_d/2} \begin{pmatrix} \bar{\mathbf{S}}_{c,11}(\xi, \xi') & \bar{\mathbf{S}}_{c,12}(\xi, \xi') \\ \bar{\mathbf{S}}_{c,21}(\xi, \xi') & \bar{\mathbf{S}}_{c,22}(\xi, \xi') \end{pmatrix} \begin{pmatrix} \bar{\boldsymbol{\psi}}^{(-)}(\xi', h_{c,1}) \\ \bar{\boldsymbol{\psi}}^{(+)}(\xi', h_{c,2}) \end{pmatrix} d\xi' \end{aligned} \tag{52}$$

with

$$\bar{\mathbf{S}}_{c,11}(\xi, \xi') = \tilde{\mathbf{B}}_c^{(+)}(\xi)\tilde{\mathbf{C}}^{-1}\tilde{\mathbf{A}}_c^{(-)}(\xi') \tag{53}$$

$$\bar{\mathbf{S}}_{c,12}(\xi, \xi') = \tilde{\mathbf{B}}_c^{(+)}(\xi)\tilde{\mathbf{C}}^{-1}\tilde{\mathbf{A}}_c^{(+)}(\xi') \tag{54}$$

$$\bar{\mathbf{S}}_{c,21}(\xi, \xi') = \tilde{\mathbf{B}}_c^{(-)}(\xi)\tilde{\mathbf{C}}^{-1}\tilde{\mathbf{A}}_c^{(-)}(\xi') \tag{55}$$

$$\bar{\mathbf{S}}_{c,22}(\xi, \xi') = \tilde{\mathbf{B}}_c^{(-)}(\xi)\,\tilde{\mathbf{C}}^{-1}\tilde{\mathbf{A}}_c^{(+)}(\xi') \tag{56}$$

$$\tilde{\mathbf{A}}_c^{(+)}(\xi) = \begin{pmatrix} \mathbf{A}^{(+)}(\xi)^t\mathbf{F}(x_{c,1}, y_{c,1} - h_{c,2}; \xi) \\ \vdots \\ \mathbf{A}^{(+)}(\xi)^t\mathbf{F}(x_{c,M}, y_{c,M} - h_{c,2}; \xi) \end{pmatrix} \tag{57}$$

$$\tilde{\mathbf{A}}_c^{(-)}(\xi) = \begin{pmatrix} \mathbf{A}^{(-)}(\xi)^t\mathbf{F}(x_{c,1}, h_{c,1} - y_{c,1}; \xi) \\ \vdots \\ \mathbf{A}^{(-)}(\xi)^t\mathbf{F}(x_{c,M}, h_{c,1} - y_{c,M}; \xi) \end{pmatrix}. \tag{58}$$

4.3. Field Decomposition

The total field $\psi(x, y)$ is here decomposed into the known incident field $\psi^{(i)}(x, y)$ and the scattered field by the periodic cylinder array without the additional cylinders $\psi^{(p)}(x, y)$, and the residual field $\psi^{(c)}(x, y)$ defined by $\psi(x, y) - \psi^{(i)}(x, y) - \psi^{(p)}(x, y)$. The decomposed fields in the surrounding medium satisfy the Helmholtz equation respectively, and the transformed fields are also expressed in the plane-wave expansions. Then the plane-wave amplitudes of the total field are expressed by the sum of the amplitudes of the decomposed fields as

$$\bar{\boldsymbol{\psi}}^{(\pm)}(\xi, y) = \bar{\boldsymbol{\psi}}^{(i,\pm)}(\xi, y) + \bar{\boldsymbol{\psi}}^{(p,\pm)}(\xi, y) + \bar{\boldsymbol{\psi}}^{(c,\pm)}(\xi, y). \tag{59}$$

Since the scattered fields consist of the outgoing waves from cylinders, $\bar{\boldsymbol{\psi}}^{(p,+)}(\xi, y)$, $\bar{\boldsymbol{\psi}}^{(p,-)}(\xi, y)$, $\bar{\boldsymbol{\psi}}^{(c,+)}(\xi, y)$, and $\bar{\boldsymbol{\psi}}^{(c,-)}(\xi, y)$ vanish in $y \leq h_{p,2}$, $y \geq h_{p,1}$, $y \leq h_{p,2}$, and $y \geq h_{c,1}$, respectively.

From Equation (33), we obtain the following relations:

$$\bar{\boldsymbol{\psi}}^{(c,+)}(\xi, h_{p,1}) = \bar{\mathbf{S}}'_{p,11}(\xi) \bar{\boldsymbol{\psi}}^{(c,-)}(\xi, h_{c,2}) \tag{60}$$

$$\bar{\boldsymbol{\psi}}^{(c,-)}(\xi, h_{p,2}) = \left(\mathbf{F}(0, h_{c,2} - h_{p,2}; \xi) + \bar{\mathbf{S}}'_{p,21}(\xi)\right) \bar{\boldsymbol{\psi}}^{(c,-)}(\xi, h_{c,2}) \tag{61}$$

with

$$\bar{\mathbf{S}}'_{p,11}(\xi) = \bar{\mathbf{S}}_{p,11}(\xi) \mathbf{F}(0, h_{c,2} - h_{p,1}; \xi) \tag{62}$$

$$\bar{\mathbf{S}}'_{p,21}(\xi) = \bar{\mathbf{S}}_{p,21}(\xi) \mathbf{F}(0, h_{c,2} - h_{p,1}; \xi), \tag{63}$$

where we have used

$$\begin{pmatrix} \bar{\boldsymbol{\psi}}^{(p,+)}(\xi, h_{p,1}) \\ \bar{\boldsymbol{\psi}}^{(p,-)}(\xi, h_{p,2}) \end{pmatrix} = \begin{pmatrix} \bar{\mathbf{S}}_{p,11}(\xi) & \bar{\mathbf{S}}_{p,12}(\xi) \\ \bar{\mathbf{S}}_{p,21}(\xi) & \bar{\mathbf{S}}_{p,22}(\xi) \end{pmatrix} \begin{pmatrix} \bar{\boldsymbol{\psi}}^{(i,-)}(\xi, h_{p,1}) \\ \bar{\boldsymbol{\psi}}^{(i,+)}(\xi, h_{p,2}) \end{pmatrix} \tag{64}$$

$$\bar{\boldsymbol{\psi}}^{(i,+)}(\xi, h_{p,1}) = \mathbf{F}(0, 2\, a_p; \xi) \bar{\boldsymbol{\psi}}^{(i,+)}(\xi, h_{p,2}) \tag{65}$$

$$\bar{\boldsymbol{\psi}}^{(i,-)}(\xi, h_{p,2}) = \mathbf{F}(0, 2\, a_p; \xi) \bar{\boldsymbol{\psi}}^{(i,-)}(\xi, h_{p,1}) \tag{66}$$

$$\bar{\boldsymbol{\psi}}^{(c,-)}(\xi, h_{p,1}) = \mathbf{F}(0, h_{c,2} - h_{p,1}; \xi) \bar{\boldsymbol{\psi}}^{(c,-)}(\xi, h_{c,2}). \tag{67}$$

Also, from Equation (52), we obtain

$$\bar{\boldsymbol{\psi}}^{(c,+)}(\xi, h_{c,1}) = \mathbf{F}(0, h_{c,1} - h_{p,1}; \xi) \bar{\boldsymbol{\psi}}^{(c,+)}(\xi, h_{p,1}) + \frac{1}{k_d} \int_{-k_d/2}^{k_d/2} \bar{\mathbf{S}}'_{c,12}(\xi, \xi') \bar{\boldsymbol{\psi}}^{(c,+)}(\xi', h_{p,1}) d\xi' + \boldsymbol{\sigma}_1(\xi) \tag{68}$$

$$\bar{\boldsymbol{\psi}}^{(c,-)}(\xi, h_{c,2}) = \frac{1}{k_d} \int_{-k_d/2}^{k_d/2} \bar{\mathbf{S}}'_{c,22}(\xi, \xi') \bar{\boldsymbol{\psi}}^{(c,+)}(\xi', h_{p,1}) d\xi' + \boldsymbol{\sigma}_2(\xi) \tag{69}$$

with

$$\begin{pmatrix}\boldsymbol{\sigma}_1(\xi)\\ \boldsymbol{\sigma}_2(\xi)\end{pmatrix} = \frac{1}{k_d}\int_{-k_d/2}^{k_d/2}\begin{pmatrix}\bar{\mathbf{S}}_{c,11}(\xi,\xi') & \bar{\mathbf{S}}'_{c,12}(\xi,\xi')\\ \bar{\mathbf{S}}_{c,21}(\xi,\xi') & \bar{\mathbf{S}}'_{c,22}(\xi,\xi')\end{pmatrix} \cdot\begin{pmatrix}\bar{\boldsymbol{\psi}}^{(i,-)}(\xi',h_{c,1})\\ \bar{\boldsymbol{\psi}}^{(i,+)}(\xi',h_{p,1})+\bar{\boldsymbol{\psi}}^{(p,+)}(\xi',h_{p,1})\end{pmatrix}d\xi' \quad (70)$$

$$\bar{\mathbf{S}}'_{c,12}(\xi,\xi') = \bar{\mathbf{S}}_{c,12}(\xi,\xi')\mathbf{F}(0,h_{c,2}-h_{p,1};\xi') \quad (71)$$

$$\bar{\mathbf{S}}'_{c,22}(\xi,\xi') = \bar{\mathbf{S}}_{c,22}(\xi,\xi')\mathbf{F}(0,h_{c,2}-h_{p,1};\xi'), \quad (72)$$

where we have used

$$\bar{\boldsymbol{\psi}}^{(i,+)}(\xi,h_{c,1}) = \mathbf{F}(0,h_{c,1}-h_{c,2};\xi)\bar{\boldsymbol{\psi}}^{(i,+)}(\xi,h_{c,2}) \quad (73)$$

$$\bar{\boldsymbol{\psi}}^{(i,-)}(\xi,h_{c,2}) = \mathbf{F}(0,h_{c,1}-h_{c,2};\xi)\bar{\boldsymbol{\psi}}^{(i,-)}(\xi,h_{c,1}) \quad (74)$$

$$\bar{\boldsymbol{\psi}}^{(p,+)}(\xi,h_{c,1}) = \mathbf{F}(0,h_{c,1}-h_{c,2};\xi)\bar{\boldsymbol{\psi}}^{(p,+)}(\xi,h_{c,2}) \quad (75)$$

$$\bar{\boldsymbol{\psi}}^{(c,+)}(\xi,h_{c,2}) = \mathbf{F}(0,h_{c,2}-h_{p,1};\xi)\bar{\boldsymbol{\psi}}^{(c,+)}(\xi,h_{p,1}). \quad (76)$$

Substituting Equations (69) into (60), we may derive the equation to be solved:

$$\bar{\boldsymbol{\psi}}^{(c,+)}(\xi,h_{p,1}) - \frac{1}{k_d}\int_{-k_d/2}^{k_d/2}\bar{\mathbf{S}}'_{p,11}(\xi)\bar{\mathbf{S}}'_{c,22}(\xi,\xi')\bar{\boldsymbol{\psi}}^{(c,+)}(\xi',h_{p,1})\,d\xi' = \bar{\mathbf{S}}'_{p,11}(\xi)\boldsymbol{\sigma}_2(\xi) \quad (77)$$

Equation (77) is the Fredholm integral equation of the second kind for $\bar{\boldsymbol{\psi}}^{(c,+)}(\xi,h_{p,1})$ to be solved and the other coefficient matrices $\bar{\boldsymbol{\psi}}^{(c,+)}(\xi,h_{c,1})$, $\bar{\boldsymbol{\psi}}^{(c,-)}(\xi,h_{c,2})$, and $\bar{\boldsymbol{\psi}}^{(c,-)}(\xi,h_{p,2})$ are then given by Equations (61), (68), and (69).

5. NUMERICAL EXPERIMENTS

When implementing a practical computation, the cylindrical-wave expansions must be truncated. We denote the truncation order for the plane-wave expansions by N that truncates the expansions from $-N$th- to Nth-order. Also, the truncation order for the cylindrical-wave expansions is denoted by K that truncates the expansions from $-K$th- to Kth-order. As the result, for example, the sizes of matrices $\tilde{\mathbf{A}}_c^{(\pm)}(\xi)$, $\tilde{\mathbf{B}}_c^{(\pm)}(\xi)$, and $\tilde{\mathbf{C}}$ become $M(2K+1)\times(2N+1)$, $(2N+1)\times M(2K+1)$, and $M(2K+1)\times M(2K+1)$, respectively. Also, the entries of matrix $\mathbf{L}(\xi)$ defined by Equation (32) are known to converge very slowly. They are called the lattice sums and direct summing does not yield effective values. An efficient calculation of lattice sums has been developed by Yasumoto and Yoshitomi [5], and the (n, m)-entries of $\mathbf{L}(\xi)$ are approximated as

$$(\mathbf{L}(\xi))_{n,m} \approx \frac{1-i}{\pi} \int_0^b G_{m-n}(\tau) \left[(-1)^{m-n} F(\tau; dk_s, d\xi) + F(\tau; dk_s, -d\xi)\right] dt \quad (78)$$

with

$$F(\tau, k', \xi') = \frac{e^{i\left(k'\sqrt{1-\tau^2}+\xi'\right)}}{\sqrt{1-\tau^2}\left[1 - e^{i\left(k'\sqrt{1-\tau^2}+\xi'\right)}\right]} \quad (79)$$

$$G_n(\tau) = \left(\tau - i\sqrt{1-\tau^2}\right)^n + \left(-\tau - i\sqrt{1-\tau^2}\right)^n \quad (80)$$

$$\tau = (1-i)t \quad (81)$$

where b is a positive constant and Equation (78) provides sufficient approximation for $b \gg 1$.

To solve Equation (77) numerically, we introduce a discretization for the transform parameter ξ. The transformed fields are periodic with the period k_d in terms of ξ as written in Section 3.1. We take therefore L sample points $\{\xi_l\}_{l=1}^L$ only in the Brillouin zone $(-k_d/2, k_d/2)$, and the integration is approximated by an appropriate numerical integration scheme. Then, Equation (77) is approximated as

$$\bar{\boldsymbol{\psi}}^{(c,+)}(\xi_l, h_{p,1}) - \sum_{l'=1}^{L} \frac{w_{l'}}{k_d} \bar{\mathbf{S}}'_{p,11}(\xi_l) \bar{\mathbf{S}}'_{c,22}(\xi_l, \xi_{l'}) \bar{\boldsymbol{\psi}}^{(c,+)}(\xi_{l'}, h_{p,1}) = \bar{\mathbf{S}}'_{p,11}(\xi_l) \boldsymbol{\sigma}_2(\xi_l) \quad (82)$$

where $\{w_l\}_{l=1}^L$ denotes the weight factor. Equation (82) can be numerically solved, and the other coefficient matrices at the sample points are obtained from Equation (61), (68), and (69) by applying the same numerical integration scheme.

Here, we consider a line source excitation problem. The line source under consideration is situated parallel to the z-axis at $(x, y) = (x_0, y_0)$ where $y_0 > h_{c,1}$ or $y_0 < h_{p,2}$. Then, the incident field is expressed as

$$\psi^{(i)}(x, y) = H_0^{(1)}(k_s \rho(x - x_0, y - y_0)). \quad (83)$$

Using the Fourier integral representation for the Hankel function of the first kind, the amplitudes of the transformed incident field are obtained as follows:

$$\left(\bar{\boldsymbol{\psi}}^{(i,+)}(\xi, y)\right)_n = \begin{cases} \frac{2}{d\beta_n(\xi)} e^{-i[\alpha_n(\xi)x_0 - \beta_n(\xi)(y-y_0)]} & \text{for} \quad y > y_0 \\ 0 & \text{for} \quad y < y_0 \end{cases} \tag{84}$$

$$\left(\bar{\boldsymbol{\psi}}^{(i,-)}(\xi, y)\right)_n = \begin{cases} 0 & \text{for} \quad y > y_0 \\ \frac{2}{d\beta_n(\xi)} e^{-i[\alpha_n(\xi)x_0 + \beta_n(\xi)(y-y_0)]} & \text{for} \quad y < y_0 \end{cases} \tag{85}$$

for integer n. Here we consider a specific example and show numerical results to validate the present formulation. The parameters are chosen as following values: $\varepsilon_s = \varepsilon_0$, $\varepsilon_p = \varepsilon_{c,m} = 4\varepsilon_0$, $\mu_s = \mu_p = \mu_{c,m} = \mu_0$, $d = 0.8\lambda_0$, $a_p = a_{c,m} = 0.4d$, and $x_p = y_p = 0$.

Figure 2 shows the obtained intensities of the total field at $(x, y) = (0, -d)$ from the structure, in which only one cylinder is located near the periodic cylinder array. The additional cylinder and the line source are located at $(x_{c,1}, y_{c,1}) = (0.5d, d)$ and $(x_0, y_0) = (0, 2d)$, respectively, and the truncation order is set to $N = K = 4$. The dotted and the dotted-dashed curves are the results of the trapezoidal rule that determines the sample points with identical interval and the constant weight. It is observed that they converge very slowly though the trapezoidal method is known to usually provide a fast convergence for the integration of smooth periodic functions over one period. The spectra for the periodic cylinder array without the additional cylinder were presented in Figure 3 of Ref. [2] and they are not smooth at the Wood-Rayleigh anomalies. The additional cylinder is thought not to change the locations of the Wood-Rayleigh anomalies, and here we use the same discretization scheme with Ref. [2], namely, the integration range is split at the Wood-Rayleigh anomalies $\xi = \pm 0.2k_d$ and the

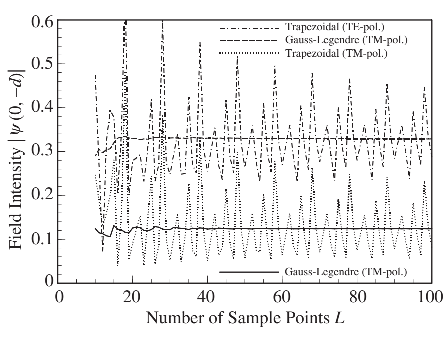

Figure 2. Convergence test of the total field intensities at $(x, y) = (0, -d)$ for one cylinder backed by periodic cylinder array with a line-source excitation as function of the number of sample points L.

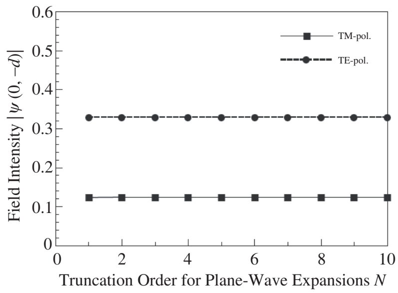

Figure 3. Same with Figure 2 but as function of the truncation order for plane-wave expansions N.

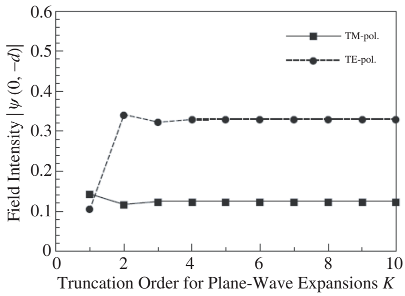

Figure 4. Same with Figure 2 but as function of the truncation order for cylindrical-wave expansions K.

sample points and weights are determined by applying the Gauss-Legendre scheme for each subinterval. The solid and the dashed curves in Figure 2 are the results and show much improvement of the convergence. The convergence in terms of the truncation order for plane-wave expansions N is shown in Figure 3. We used $L = 60$ and $K = 4$, and the sample points and the weights are determined by the Gauss-Legendre scheme applying to the subintervals. The convergence is very fast, and this implies that the analysis region can be limited in the wavenumber space for practical computation. The numerical results of the convergence test in terms of the truncation order for cylindrical-wave expansions K are shown in Figure 4. They are calculated with $L = 60$ and $N = 4$, and the discretization scheme is same with Figure 3. We examine the reciprocal property to validate the present formulation. Let $\psi_{pq}(x_p, y_p; x_q, y_q)$ be the field observed at (x_p, y_p) for a line source located at (x_q, y_q). Then we define the reciprocity error by

$$\sigma(x_p, y_p; x_q, y_q) = \frac{|\psi_{pq}(x_p, y_p; x_q, y_q) - \psi_{qp}(x_q, y_q; x_p, y_p)|}{|\psi_{pq}(x_p, y_p; x_q, y_q)|}. \tag{86}$$

The reciprocity theorem requires that this function is zero when both (x_p, y_p) and (x_q, y_q) are not located in $h_{p,2} < y < h_{c,1}$. We fix one point $(x_q, y_q) = (0, 2d)$ and the other point (x_p, y_p) is moved on the line $y = 1.5d$. Figure 5 shows calculated values of $\sigma(x, 1.5d; 0, 2d)$ at 101 points with identical intervals in $-4d \leq x \leq 4d$, where we calculated in the standard double-precision arithmetic. The largest value is about 3.3×10^{-13}, and the reciprocity relation is well satisfied. Also, the results of the present formulation are compared with those of the conventional RTMA [3] for the scattering from a finite number of

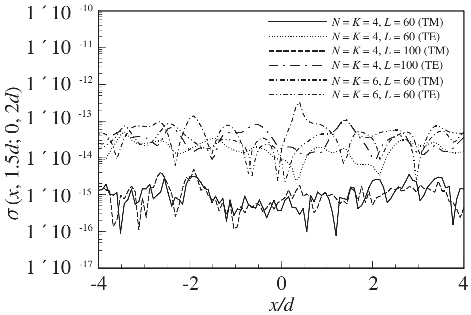

Figure 5. Numerical results of reciprocity test for one cylinder backed by periodic cylinder array with a line-source excitation.

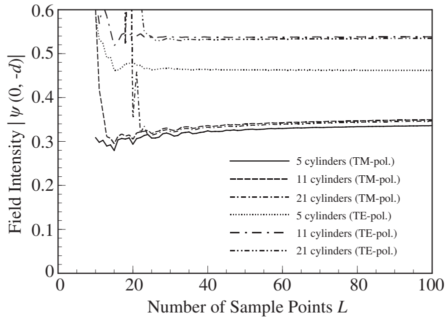

Figure 6. Convergence test of the total field intensities at $(x, y) = (0, -d)$ for several cylinders backed by periodic cylinder array with a line-source excitation as function of the number of sample points L.

cylinders. From the physical point of view, if the number of cylinders is large enough, the fields near the line source is expected not to be noticeably different in both methods. Here, we consider 201 cylinders located at $(x, y) = (md, 0)$ for $m = 0, \pm 1, \dots, \pm 100$, and the intensity of the total field at $(x, y) = (0, -d)$ is calculated by the conventional RTMA. The obtained values are 0.3031 for TM-polarization and 0.1134 for TE-polarization, which are in good agreement with the results of the present formulation.

Numerical results of the convergence tests for finite sets of parallel cylinders placed near the periodic cylinder array are shown in Figures 6–8. The numbers of additional cylinders are set to $M = 5$, 11, 21, and the cylinders are located on the line $y = d$ with identical intervals. We set the position of the mth-cylinder $(m = 1, \dots, M)$ as $(x_{c,m}, y_{c,m}) = ([m - (M + 1)/2]d_c, d)$ with $d_c = 1.3d$. It is observed

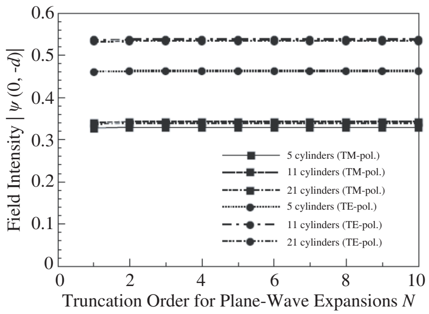

Figure 7. Same with Figure 6 but as function of the truncation order for plane-wave expansions N.

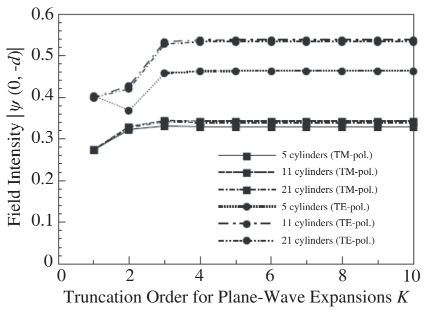

Figure 8. Same with Figure 6 but as function of the truncation order for cylindrical-wave expansions K.

that the convergence speed is similar to the one cylinder case and the number of additional cylinder seems not to affect a lot to the convergence speed.

6. CONCLUSIONS

This paper has formulated the two-dimensional electromagnetic scattering problem of an imperfectly periodic structure, in which circular cylinders are located near a periodic array consisting of circular cylinders. The present formulation is based on the multilayer technique with the help of PPFT, and RTMA with the lattice sums technique is also used to treat adequately the boundary conditions at the cylinder surfaces. PPFT introduces the transform parameter ξ, which is related to the wavenumber, and the transformed fields have a periodic property in terms of ξ. The practical computation requires an appropriate discretization on ξ in the Brillouin zone. However, since the Wood-Rayleigh anomalies are degenerated to two points in the Brillouin zone and the discretization scheme is comparatively easy to consider. The numerical results of convergence and reciprocal tests verified the present formulation, and the number of additional cylinder seems not to greatly influence the convergence speed.

REFERENCES

1. Petit, R., ed., *Electromagnetic Theory of Gratings*, Springer Verlag, Berlin, 1980.

2. Watanabe, K. and K. Yasumoto, "Two-dimensional electromagnetic scattering of non-plane incident waves by periodic structures," *Progress In Electromagnetics Research*, Vol. 74, 241–271, 2007.
3. Chew, W. C., *Waves and Fields in Inhomogeneous Media*, Van Nostrand Reinhold, New York, 1990.
4. Roussel, H., W. C. Chew, F. Jouvie, and W. Tabbara, "Electromagnetic scattering from dielectric and magnetic gratings of fibers — a T-matrix solution," *Journal of Electromagnetic Waves and Applications*, Vol. 10, No. 1, 109–127, 1996.
5. Yasumoto, K. and K. Yoshitomi, "Efficient calculation of lattice sums for free-space periodic Green's function," *IEEE Trans. Antennas Propagat.*, Vol. 47, No. 6, 1050–1055, 1999.
6. Abramowitz, M. and I. Stegun, ed., *Handbook of Mathematical Functions with Formulas, Graphs, and Mathematical Tables*, Dover, New York, 1972.